



Accumulated deformation and microstructure of deep silty clay subjected to two freezing-thawing cycles under cyclic loading

Chen-Yu Hou¹ · Zhen-Dong Cui¹ · Li Yuan¹

Received: 15 July 2019 / Accepted: 6 May 2020 / Published online: 10 June 2020
© Saudi Society for Geosciences 2020

Abstract

The problem of the settlement and deformation of soft clay is becoming more and more prominent under the subway vibration loading. Due to the complexity of the construction environment in the soft soil areas, the artificial freezing method is often used to reinforce the soil, and sometimes it is also subjected to twice freezing. The Shanghai subway line crosses vertically and horizontally. The deepest excavation depth reaches 33.1 m, so the construction of the subway tunnel will develop to a deeper stratum. In this paper, the GDS dynamic triaxial tests were conducted to study the accumulated deformation of the gray silty clay of layer no.8 in Shanghai, 60 m in depth. Considering the influence of vibration time, frequencies, freezing temperatures, and freezing-thawing cycles, the axial strain of the deep silty clay before and after freezing-thawing was analyzed. The results show that the strain of the soil subjected to one freezing-thawing cycle and two freezing-thawing cycles increases by 39.6% and 72.8% comparing with the unfrozen soil, respectively. With the increase of vibration time, the rates of increasing of the axial strain gradually decrease. The higher the frequency and the lower the freezing temperature, the more deformation produces to the soil. The microstructures of the soil before and after freezing-thawing were obtained by mercury intrusion porosimetry (MIP) tests. There is a bottleneck with the pressure about 100 psi in the mercury intrusion process. Under the same cyclic loading, the lower the freezing temperatures and the more the freezing-thawing cycles, the more the mercury intrusion volume and the cumulative pore area. The most probable pore diameter of the unfrozen soil is about 524 nm smaller than that of the thawing soil, which is about 1050 nm. The pores 10–100 nm in diameter account for a large part. This research is of great guiding significance for the construction of deep subway tunnels.

Keywords Deep silty clay · Dynamic characteristics · Freezing-thawing · Accumulated deformation · MIP tests · Pore size distribution

Introduction

With the rapid development of urban rail transit, the excavation depth of subway tunnels will be larger and larger. There are 14 three-line interchange stations and one four-line interchange station in Shanghai and the largest depth of the station reaches 33.1 m. Due to the low permeability, high water content, and high compressibility of the soft clay, the settlement and

deformation of the soft soil foundation caused by the continuous subway vibration loading become increasingly prominent.

Artificial freezing method is to reduce the temperature of natural soil to form ice by using artificial refrigeration technology so that the soil can be transformed into frozen soil with higher strength and better stability. As the ground water is isolated from the construction, the safety of the project is improved (Li et al. 2015). Due to high water content, low strength, and high compressibility of soft soil (Ling et al. 2013), the artificial freezing method becomes one of the main construction methods of subway tunnel and cross passage. After freezing and thawing, the soil particle structure will change. In addition, the physical and mechanical properties are different with those of the undisturbed soil (Chamberlain and Gow 1979). Eigenbrod found that the soil volume changed the most in the first freeze-thaw cycle, and the permeabilities of the soil increased (Eigenbord 1996). There was a significant decrease for the resilient modulus of the cohesive soil during the freezing-thawing process (Lee et al. 1995). Simonsen

This paper was selected from the 1st Conference of the Arabian Journal of Geosciences (CAJG), Tunisia 2018

✉ Zhen-Dong Cui

¹ State Key Laboratory for Geomechanics and Deep Underground Engineering, School of Mechanics and Civil Engineering, China University of Mining and Technology, Xuzhou 221116, Jiangsu, People's Republic of China

pointed out that the degree of the attenuation of the resilient modulus was related to the nature of the soil (Simonsen et al. 2002). Under the cyclic loading, there occurred obvious settlement for the thawing soil and the more freezing-thawing cycles, the more cumulative strain. With the dynamic stress amplitude increasing, the cumulative strain increased. But it decreased with the increase of the confining pressure (Lin et al. 2017). Tang founded that after fully freezing-thawing, the uniaxial compressive strength of the soil increased (Tang et al. 2012). The thawing soil became looser and its elastic modulus decreased with the strain increasing (Cui et al. 2014). What is more, the unconfined compressive strength decreases with the increase of the freezing-thawing cycles, and the volume of the soil changes the most in the first freezing-thawing cycle (Kamei et al. 2012).

By the consecutive dynamic field monitoring, the soil response frequency caused by the subway vibration was divided into high frequency (2.4–2.8 Hz) and low frequency (0.4–0.6 Hz) (Tang et al. 2008). Under the subway vibration, the deformation of the soft clay was rapidly developed in the initial stage, and the cyclic stress ratio is the main influencing factor (Yan et al. 2012). Shen also got similar conclusion in the field measurements (Shen et al. 2014). After the freezing-thawing cycle, the development of the axial strain was similar to the undisturbed soil, it increased with the increase of the vibration frequency and the cyclic stress ratio, and the excess pore pressure and damping ratio also increased. The shear modulus and excess pore pressure increased as the freezing temperature decreasing (Cui and Zhang 2015; Zhang and Cui 2018a). Under long-term cyclic loading, the elastic modulus decreased with the loading cycles increasing. It became stable when reaching 50,000 cycles, and the larger the CSR, the more loading cycles were required (Guo et al. 2013). The damping ratio decreased and the stiffness increased with the increasing of the loading cycles. And their development was associated with the accumulative strain (Ling et al. 2013). As the depth increases, the physical and mechanical properties of the soil change significantly. The hydraulic properties of the soil buried in the deep environments are more complicated comparing with those in the shallow condition (Zhou et al. 2018). The deep soil experiences a long period of geological history under high pressure. The shear tests and SEM tests were carried out by Ma to study the decreasing strength phenomenon in the frozen soils subjected to high confining pressures, and the main reasons were the increase of microcracks and the pressure melting of pore ice (Ma et al. 1999). Yoichi studied the undrained shear strength of Pleistocene Clay in Osaka Bay from depths of 20–200 m; the results showed that the shear strength and consolidation yield stress had a growth trend with depth (Watabe et al. 2002).

Since the birth of the new testing techniques such as the polarizing microscopy, the scanning electron microscopy, the mercury intrusion porosimetry, and the X-ray diffraction, many researchers began to study the vibration of the microstructures. Among these technologies, the MIP is frequently

used to qualitatively evaluate the pore size distribution of the soils (Penumadu and Dean 2000). There was a bottleneck effect in the intrusion stage of the MIP test, and the soil structures in different layers were different (Cui and Tang 2011). What is more, the segregation freezing caused the change of the soil. The pore area and the void ratio both decreased after freezing-thawing (Tang and Yan 2014). You studied the microstructure of the frozen silty clay by SEM and MIP tests. Based on the results, the porosity increased firstly and then decreased with the increasing of the salt content. It was believed that the salt in the soil changed the volume of the pores, not the soil particles (You et al. 2017). However, Zhang indicated that the water in the saturated soil turning into ice caused the volume expansion, and the mercury intrusion volume increased with the decreasing of the freezing temperature (Zhang and Cui 2018b). Also, with the increase in the depth of the soil, the pore diameter and mercury intrusion decreased. And the bottleneck effect was caused by the hysteresis of the soil samples (Cui et al. 2016).

It can be seen that there are many researches on the dynamic properties of the silty clay under the subway vibration. But the studies on the deep clay are very few, and the physical and mechanical properties of the deep soils are also very complex. Therefore, the main research of this paper is to study the mechanical properties and microscope pore structures of the deep silty clay after freezing-thawing cycle under the subway vibration. The dynamic triaxial tests of the silty clay of layer no. 8 in Shanghai were conducted to study the effect of the frequencies, the freezing temperatures, and the freezing-thawing cycles. Also, the vibration of the microstructures in different freezing temperatures and freezing-thawing cycles was analyzed. This research is of great significance to the construction of the deep subway tunnels.

Test methods

Test material

The soil samples were obtained from the gray silty clay of layer no. 8 in Shanghai (about 59–64 m in depth). The lithology of the clay is mainly gray silty clay interbedded with thin silty sand sublayer, gray silty clay, and gray silty sand interlayer. In order to ensure the sealing of the soil samples, the soils were put in the metal cylinders wrapped with paraffin and plastic film. The inner diameter of the metal cylinder is 100 mm and the height is 300 mm. Then the samples were placed in a wet room to prevent water loss. In this research, three different freezing temperatures – 10 °C, – 20 °C, and – 30 °C were set to freeze the soil samples in the freezing box. The freezing time was converted to the actual project to make the test closer to the engineering practice, which was 48 h. After freezing, the soil samples were placed in the constant temperature and humidity oven for thawing. This process was one freezing-thawing cycle, and the two freezing-

Table 1 Physical properties of the silty clay samples

Soils	Water content (%)	Initial density (g/cm^3)	Initial void ratio	Liquid limit	Plastic limit	Cohesion (kPa)	Internal friction angle ($^\circ$)
U	38.79	1.88	1.001	37.1	22.4	15.8	14.5
F	39.96	1.85	1.048	38.4	22.3	16.3	14.3
2F	40.38	1.83	1.093	39.2	22.1	16.9	13.9

thawing cycles were similar. The properties of the silty clay are summarized in Table 1. Figure 1 presents the soil sample of dynamic triaxial test.

The dynamic triaxial test

In this paper, the sine wave and one-way stress controlled cyclic loading were chosen to conduct the dynamic triaxial test. Thirteen samples in this test were prepared to a diameter of 38 mm and a height of 76 mm in accordance with the requirements of China Nation Standard. The samples were saturated with 3 grade back pressures and B value > 0.95 . In order to perfectly simulate the stress state of the site, the samples were consolidated under the condition of K_0 . The axial stress applied to the soil was calculated by the layer-wise summation method. After calculation, the axial stress was 1120 kPa, the confining pressure was 960 kPa, and the back pressure was 420 kPa. The dynamic stress amplitude was assumed as 40 kPa, and the cyclic stress ratio, $\text{CSR} = q_d/2p_0$, where q_d is the dynamic stress amplitude and p_0 is effective confining pressure. Then three different frequencies of subway vibration 0.5 Hz, 1.5 Hz, and 2.5 Hz were selected according to the monitoring data of Shanghai Metro. The loading time of each sample was 2 h, and the tests were undrained.

The MIP test

The MIP tests were conducted using Micromeritics Auto Pore 9500 automatic mercury intrusion porosimeter. The

mercury intrusion instrument consists of one high-pressure station and two low-pressure stations, reaching a maximum pressure of 228 MPa (33,000 psi). And the measurable pore size ranges from 0.003 to 1000 μm . The principle of the mercury intrusion test is that mercury is nonwetting to most solid materials and has a liquid-specific surface tension. The intrusion pressure is inversely proportional to the equivalent pore entry diameter. Based on the assumption of a cylinder with a constant radius proposed by Washburn, there is an equation between the pore diameter and intrusion pressure:

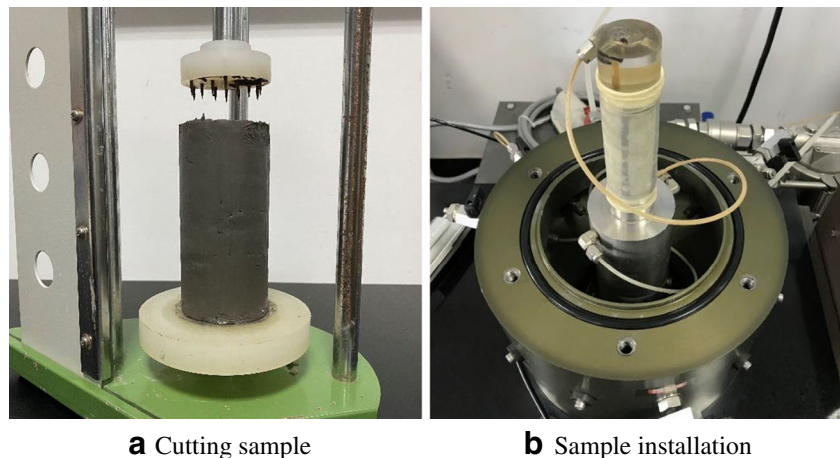
$$r = -\frac{2\gamma\cos\theta}{p} \quad (1)$$

where p is intrusion pressure, r is radius of the pore, θ is the contact angle between mercury and soil interface which has the value of 140° in this study, and γ being the surface tension of mercury which has the value of 0.485 N/m.

By the increasing of the intrusion pressure from p to Δp , more mercury will enter into the pores, and the corresponding pore radius filled by mercury will decrease from r to Δr , and the volume pore size distribution function $D_V(r)$, defined as the pore volume per unit interval of pore radius, gives the following:

$$D_V(r) = -\frac{p}{r} \left(\frac{dV}{dp} \right) \quad (2)$$

Fig. 1 Soil sample of dynamic triaxial test



a Cutting sample

b Sample installation

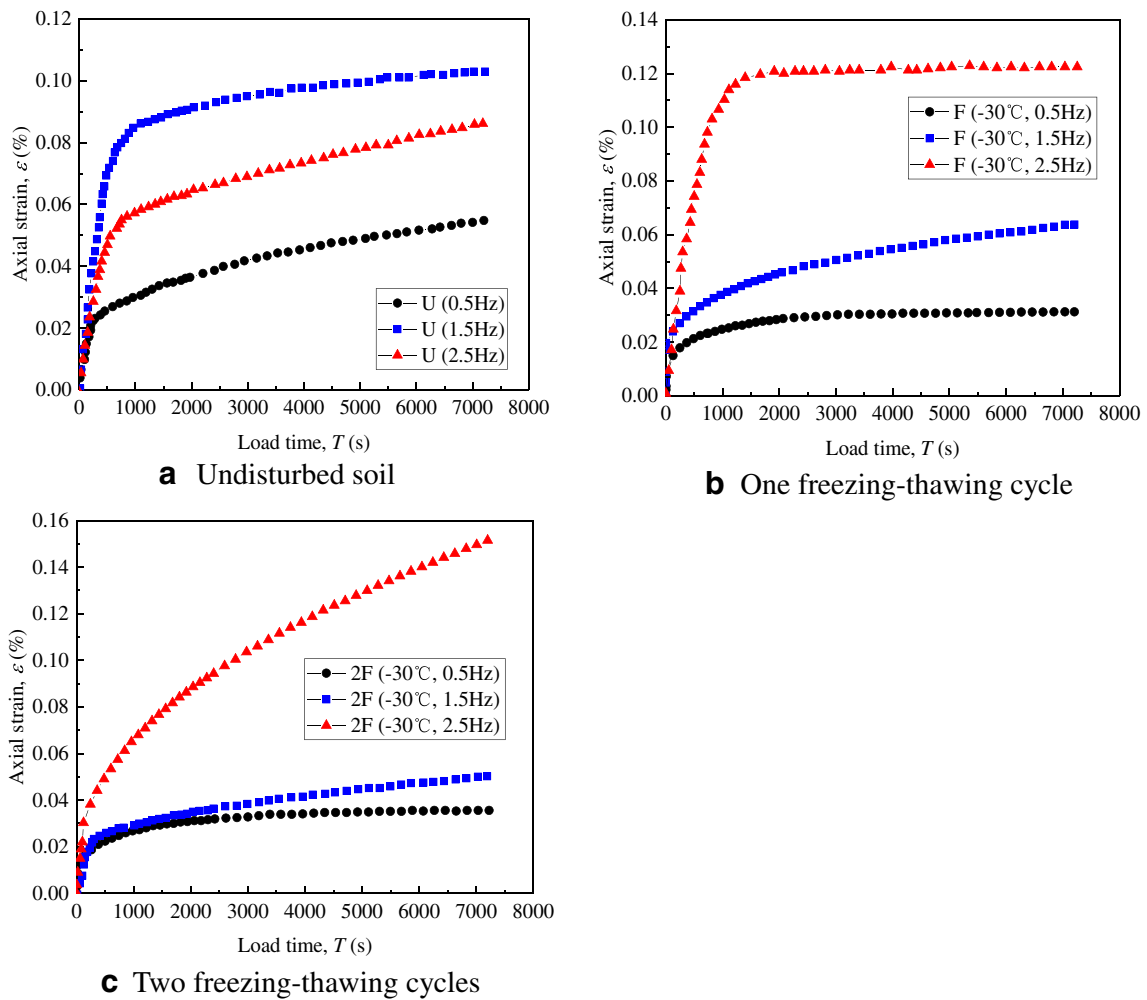


Fig. 2 Axial strain and loading time curves at different frequencies. **a** Undisturbed soil. **b** One freezing-thawing cycle. **c** Two freezing-thawing cycles

where D_V is the volume pore size distribution function, defined as the pore volume per unit interval of pore radius. The volume log radius distribution function $D_V(\log r)$ can be expressed as follows:

$$D_V(\log r) = \frac{dV}{d\log r} = rD_V(r) \tag{3}$$

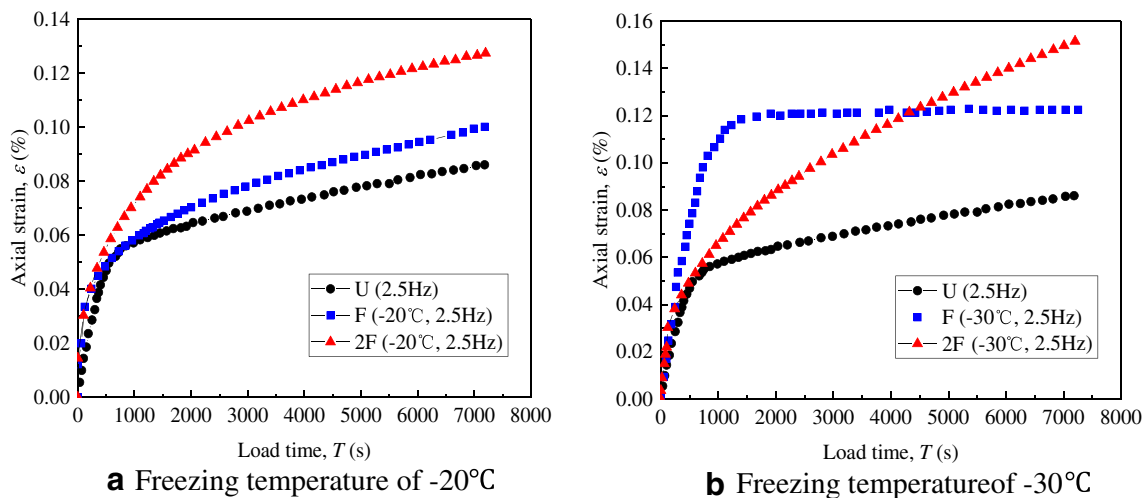


Fig. 3 Axial strain and loading time curves at different freezing-thawing cycles. **a** Freezing temperature of -20 °C. **b** Freezing temperature of -30 °C

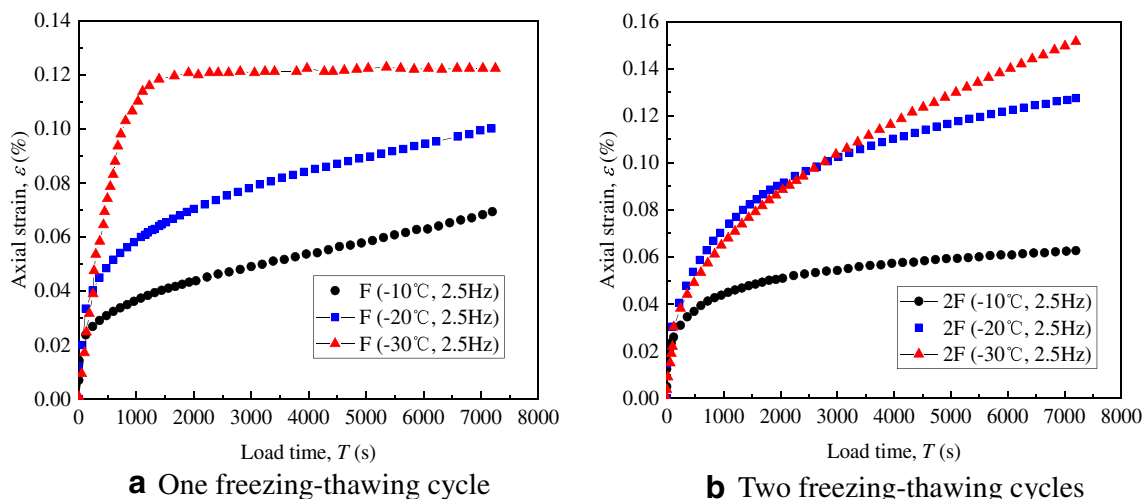


Fig. 4 Axial strain and loading time curves at different freezing temperatures. a One freezing-thawing cycle. b Two freezing-thawing cycles

Combining Eq. (3) with Eq. (2) gives the following:

$$D_V(\log r) = -p \frac{dV}{dp} = -\frac{dV}{d \log p} \tag{4}$$

Samples preparing and test procedure are as follows:

- (1) Carefully remove the loaded sample from the test device. Cut the outer rubber film with scissors.
- (2) Cut a wedge notch with a sharp blade along the height of the sample. Incise the middle part of the sample into a strip of 10 × 10 × 20 mm (length × width × height).
- (3) Put the samples into the liquid nitrogen and immediately freeze. Then place them in the vacuum freeze-drying machine for complete drying.
- (4) Analytically weigh the samples and put them in the dilatometer, which are then assembled and inserted into the low-pressure station for intrusion.

- (5) After low-pressure intrusion, weigh the samples and dilatometer again, and then put into the high-pressure station for intrusion.
- (6) After high-pressure intrusion, analyze the results and dispose the remaining mercury.

Test results and analysis

Analysis of the accumulated deformation

Under cyclic loading, the accumulated deformation of the soft clay is affected by many factors. The main reason is the change of the internal structure of the soil. The larger the internal pore volume, the easier the soft clay is compressed and the greater the deformation (Pillai et al. 2011). The accumulated strain during

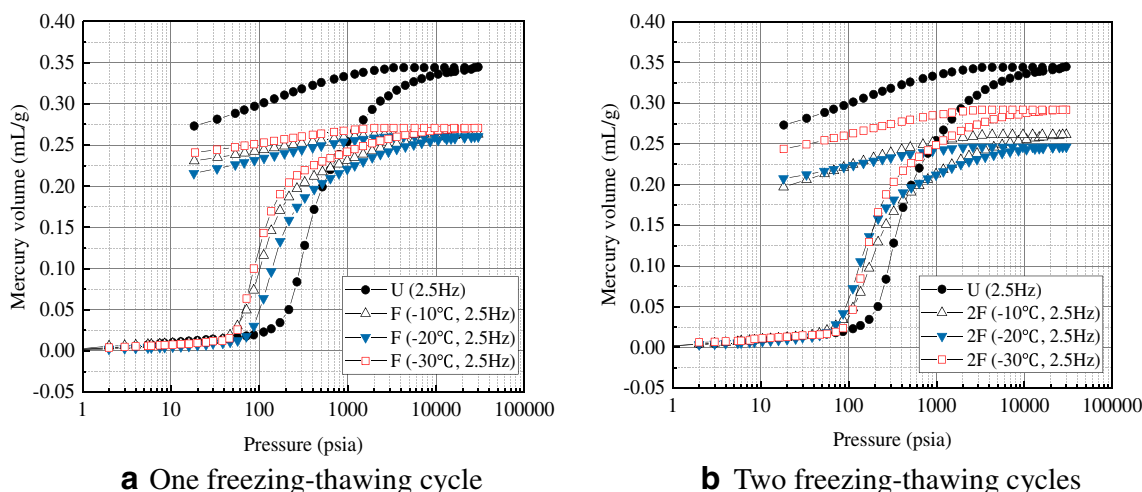


Fig. 5 The intrusion and extrusion curves at different freezing temperatures. a One freezing-thawing cycle. b Two freezing-thawing cycles

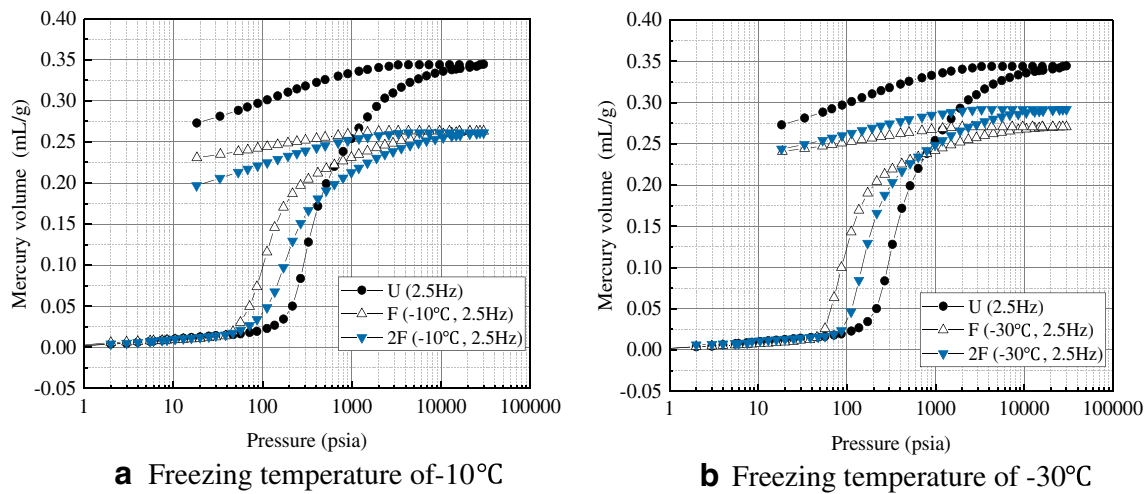


Fig. 6 The intrusion and extrusion curves at different freezing-thawing cycles. **a** Freezing temperature of $-10\text{ }^{\circ}\text{C}$. **b** Freezing temperature of $-30\text{ }^{\circ}\text{C}$

the cyclic triaxial tests is almost the plastic strain; the elastic strain is very little. The variations of the accumulated strain can be divided into three stages: the sharply increasing stage, the slowly stable stage, and the smooth stage. And the deformation in the initial stage is very obvious (Tang et al. 2012). In this research, the loading time, frequency, and number of freezing-thawing cycles are considered as the influencing factors of the accumulated deformation. The loading time of each sample with different frequencies is the same, which is 7200 s.

Figure 2 illustrates the axial strain and loading-time curves with different frequencies. It can be seen that in the initial stage, the axial strain develops the most with a rapid increasing rate, when the loading time is about 1000 s, the curves gradually become gentle. In general, the axial strain increases with the increasing of the loading time. The axial strain curves subjected to one freezing-thawing cycle with freezing temperature of $-30\text{ }^{\circ}\text{C}$ are shown in Fig. 2b, and we can see that the axial strain of the sample with vibration frequency 0.5 Hz is about 0.03%, while the samples with frequency

1.5 Hz and 2.5 Hz have larger deformation, which is about 0.06% and 0.12%. It is obvious that the frequency has a great effect on the accumulated deformation. The samples with higher frequency will produce larger axial strain. Because at the same loading time, the higher the frequency, the more number of the vibrations of the cyclic loading is passed to the soil, and the more energy transfers to the soil which contributes to the deformation.

The axial strain and loading-time curves at different freezing-thawing cycles are presented in Fig. 3. At the same vibration frequency of 2.5 Hz, the freezing-thawing samples have larger axial strain comparing with the undisturbed soil, which is about 0.10% and 0.12% with freezing temperature $-20\text{ }^{\circ}\text{C}$ and $-30\text{ }^{\circ}\text{C}$. After freezing, the water in the pores of the soil turns into ice, resulting in the increase of the pore volume, so the deformation becomes larger than the undisturbed soil. In Fig. 3 a, the strain of the soil with frequency 2.5 Hz and freezing temperature $-20\text{ }^{\circ}\text{C}$ subjected to one freezing-thawing cycle increases by 39.63% comparing with the undisturbed soil, and the strain subjected to

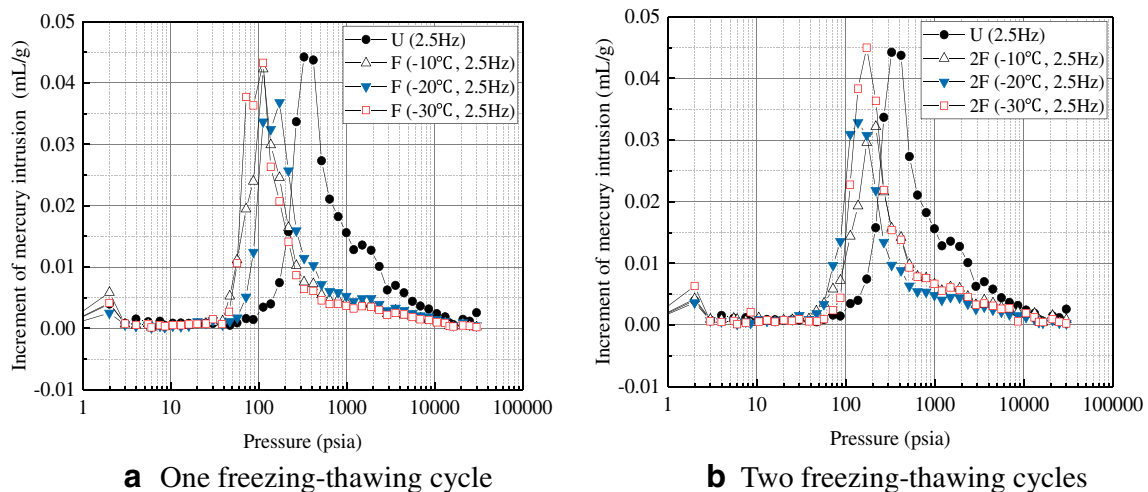


Fig. 7 The increment of mercury intrusion curves at different freezing temperatures. **a** One freezing-thawing cycle. **b** Two freezing-thawing cycles

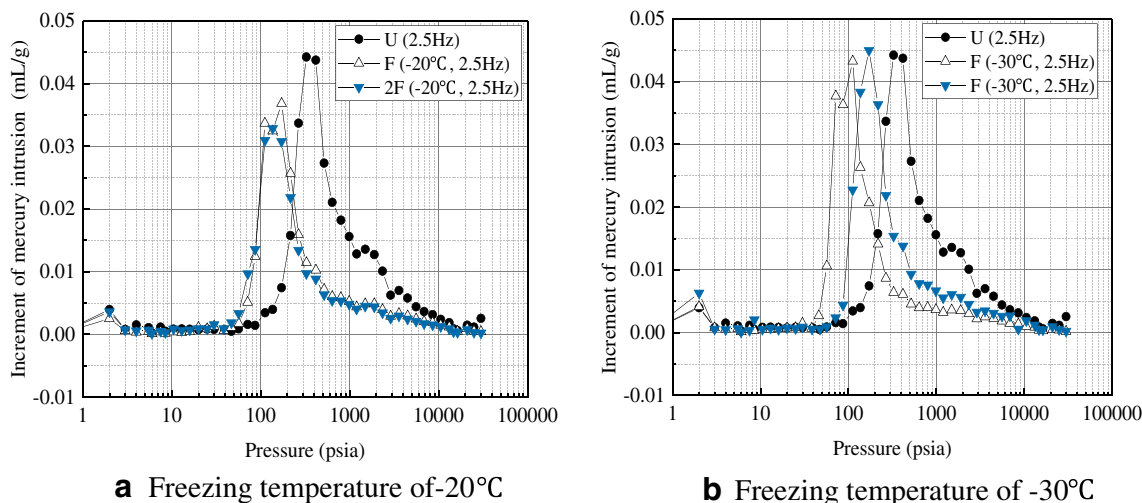


Fig. 8 The increment of mercury intrusion curves at different freezing-thawing cycles. **a** Freezing temperature of $-20\text{ }^{\circ}\text{C}$. **b** Freezing temperature of $-30\text{ }^{\circ}\text{C}$

two freezing-thawing cycles increases by 72.81%. It is obvious that the larger number of the freezing-thawing cycles, the more accumulated deformation of the soil. This is consistent with the conclusion reached by Lin et al. (2017). After freezing-thawing, the volume of water in the pores expands, and the joint between the internal structures of the soil is destroyed. The tiny pores penetrate each other to form into larger pores, which increases the pore volume of the soil. The soil is compressed under the subway vibration.

Figure 4 shows the variations of the axial strain at different freezing temperatures. It can be seen from the figures that the influence of freezing temperature on the development of the strain is also obvious. The lower the freezing temperature, the larger the axial strain. The soil with the freezing temperature of $-30\text{ }^{\circ}\text{C}$ produces the largest strain. For the samples of one freezing-thawing cycle, the axial strain is about 0.07% with freezing temperature $-10\text{ }^{\circ}\text{C}$, and the deformation of the samples with freezing temperature of $-20\text{ }^{\circ}\text{C}$ and $-30\text{ }^{\circ}\text{C}$ is about 0.10% and 0.12%. Figure 4 b presents the accumulated

deformation of the soil subjected to two freezing-thawing cycles. The axial strain of the sample at freezing temperature $-20\text{ }^{\circ}\text{C}$ increased by 103.35% than that of the freezing temperature $-10\text{ }^{\circ}\text{C}$, and the axial strain of freezing temperature $-30\text{ }^{\circ}\text{C}$ increased by 153.33%. The frost heaving appears under the action of freezing-thawing; the lower the freezing temperature, the more obvious the frost heaving effect. The penetration of the micropores increases the number of large pores, and the damage of the internal structure in the soil increases. Under cyclic loading, the pores in the soil are compressed, which resulting in the accumulated plastic strain. Thus, it can be seen that the freezing temperature has a great effect on the accumulated deformation.

Analysis of the microscope pore structure

A series of MIP tests were conducted to study the pore size distribution (PSD) of the deep silty clay under different freezing-thawing cycles and freezing temperatures. Figure 5

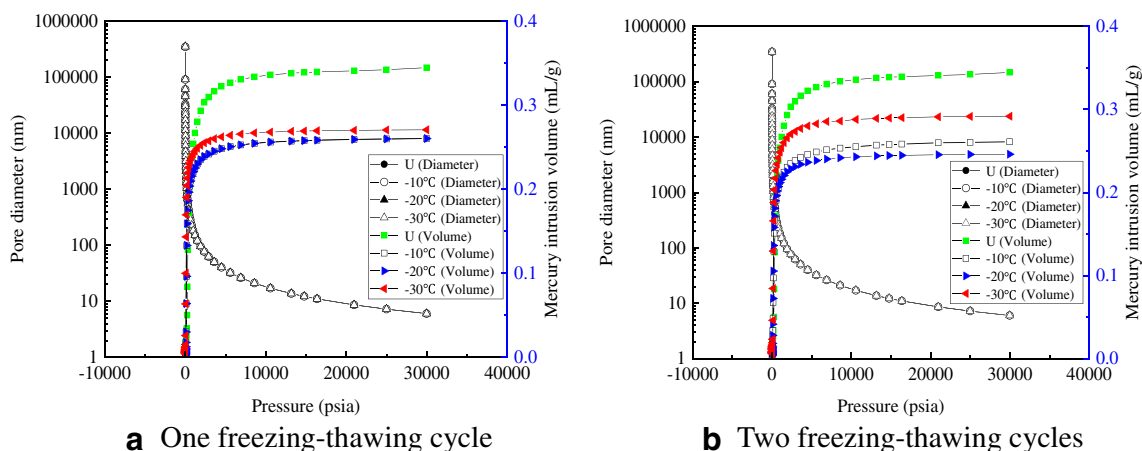


Fig. 9 The pore diameter and volume curves at different freezing temperatures. **a** One freezing-thawing cycle. **b** Two freezing-thawing cycles

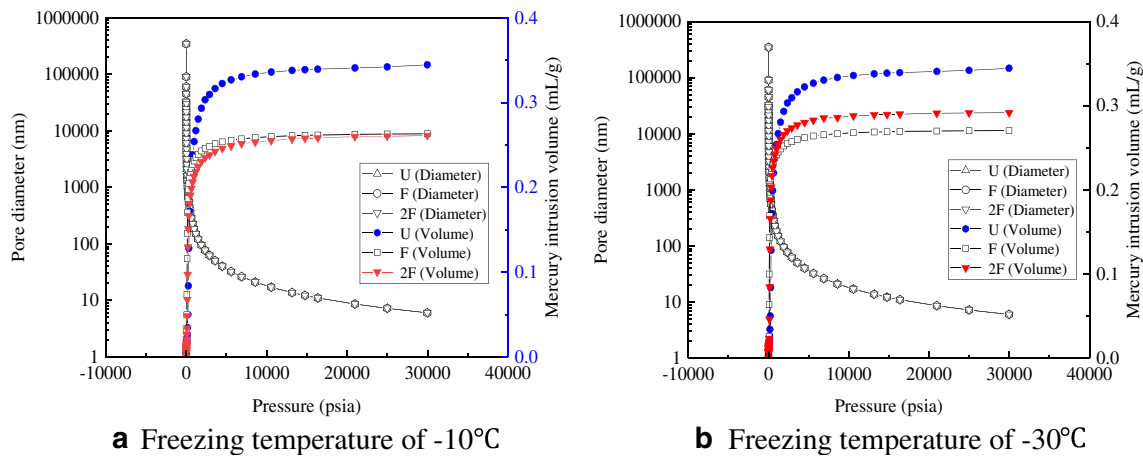


Fig. 10 The pore diameter and volume curves at different freezing-thawing cycles. **a** Freezing temperature of -10°C . **b** Freezing temperature of -30°C

shows the intrusion and extrusion curves with different freezing temperatures. With the increase of pressure, the mercury entering the pores of the soil increases, at the low-pressure stage and the initial stage of high pressure, the volume of mercury is very small. When the pressure reaches about 100 psi, the mercury fills the pores rapidly. This shows that there is a bottleneck in the entering process of mercury, after the neck, the mercury will increase rapidly and rise to a large value at a small increment of pressure (Cui and Tang 2011). It can be seen from Figs. 5 and 6 that the intrusion and extrusion curves are not closed, and the hysteresis effect of micropores and small pores in the soil results in the retention of mercury.

The mercury intrusion and extrusion curves reflect the increase and decrease of mercury intake with the mercury injection pressure. Under the same loading condition, the intrusion and extrusion curves of undisturbed soil and thawing soil are different, as shown in Fig. 5. The mercury intrusion curves are close to each other before the pressure reaches 100 psi. And the final volume of mercury intrusion increases with the decrease of

freezing temperature. Because the lower the freezing temperature, the more water in the pores will freeze to ice, which increases the volume of pores, and the mercury intrusion volume will be larger. Figure 5 shows the intrusion and extrusion curves with different freezing-thawing cycles under same loading condition. It can be seen that the mercury intrusion volume subjected to two freezing-thawing cycles is larger than the one freezing-thawing cycle. The effect of the frost heave of two freezing-thawing cycles is more obvious and the pore volume is larger comparing with that of the one freezing-thawing cycle.

The increment of mercury intrusion under different pressure indicates the pore volume and pore size of soil under a certain pressure. Figure 7 presents the increment of mercury intrusion curves at different freezing temperatures. As the pressure increases, the increment of mercury intrusion increases slowly at the beginning. When reaches about 100 psi, the increment of mercury intrusion increases rapidly and reaches the peak value, finally the increment gradually decreases and tends to be gentle. The increment of mercury intrusion is corresponding to the slope

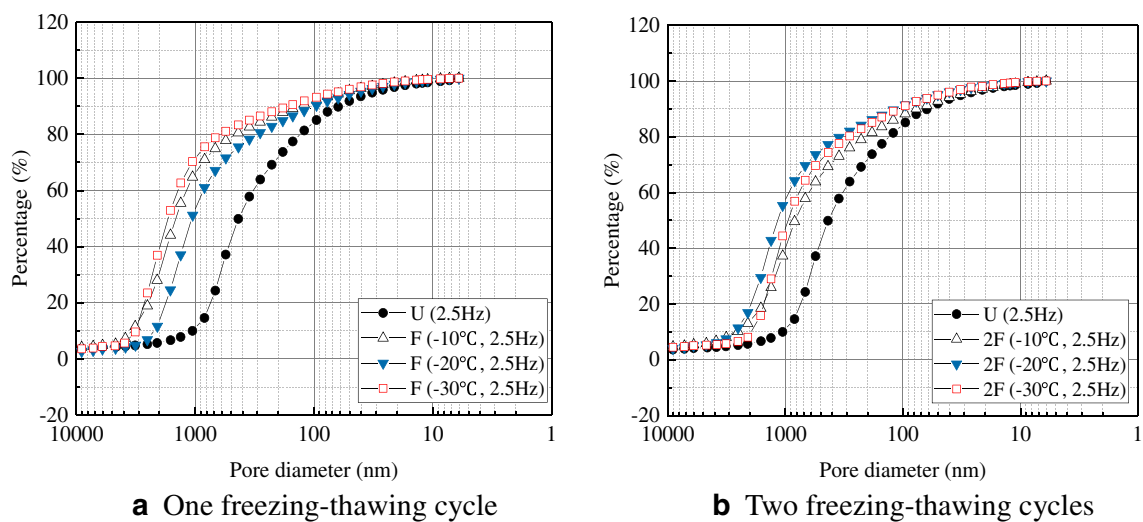


Fig. 11 Percentage of pore volume greater than a certain pore diameter curves at different freezing temperatures. **a** One freezing-thawing cycle. **b** Two freezing-thawing cycles

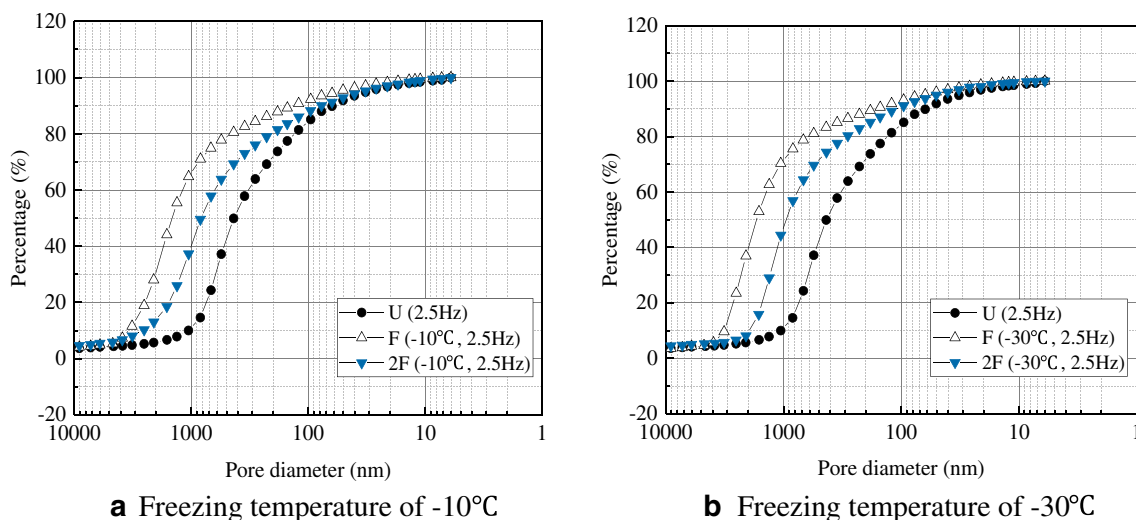


Fig. 12 Percentage of pore volume greater than a certain pore diameter curves at different freezing-thawing cycles. **a** Freezing temperature of $-10\text{ }^{\circ}\text{C}$. **b** Freezing temperature of $-30\text{ }^{\circ}\text{C}$

in the intrusion and extrusion curve, which indicates the growth rate of the mercury volume. The peak value corresponding to the mercury intrusion pressure of the undisturbed soil is larger than the thawing soil. According to Eq. (1), it can be seen that the higher the pressure, the smaller the pore diameter, so the pore diameter of the undisturbed soil is smaller than the thawing soil. Also, the peak value increases with the freezing temperature decreasing, this is because the lower the freezing temperature, the larger the pore volume of the soil, and the number of the large pores also increases. Figure 8 shows the increment of mercury intrusion curves with different freezing-thawing cycles. It shows that the increment of mercury intrusion subjected to two freezing-thawing cycles is larger than one freezing-thawing cycle.

The relationship between soil pore size and mercury intrusion pressure obtained in MIP tests is called mercury injection curve. Figure 9 illustrates the pore diameter and volume curves at different freezing temperatures. It can be seen that the diameter and

pressure curves are almost the same, showing an L shape. This is because the soil samples of the MIP test are the same, so the pore diameter of the soil corresponding to different mercury intrusion pressures is the same. As the increase of the pressure, the pore diameter gradually decreases. The mercury is rapidly filled into the pores with large diameters at the low intrusion pressure, the pores with small diameters need higher mercury intrusion pressure and the mercury is not easy to enter, so as the pore diameter decreases, the mercury intrusion pressure increases. This indicates that there are many small pores in the soil, although the pore diameter is small, the amount of pores is large. Figure 8 also shows that the final mercury intrusion volume increases with the decrease of freezing temperatures. The pore diameter and volume curves at different freezing-thawing cycles are shown in Fig. 10; the curves of frozen soils are close to each other.

According to the proportion of different pores to the total pore volume in the soil sample, the distribution of pores with

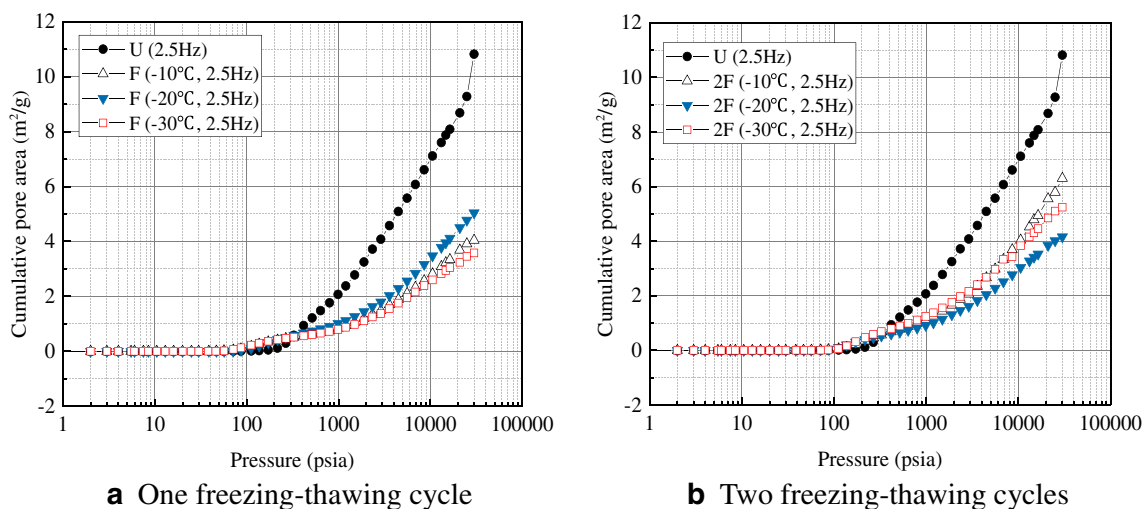


Fig. 13 The cumulative pore area curves at different freezing temperatures. **a** One freezing-thawing cycle. **b** Two freezing-thawing cycles

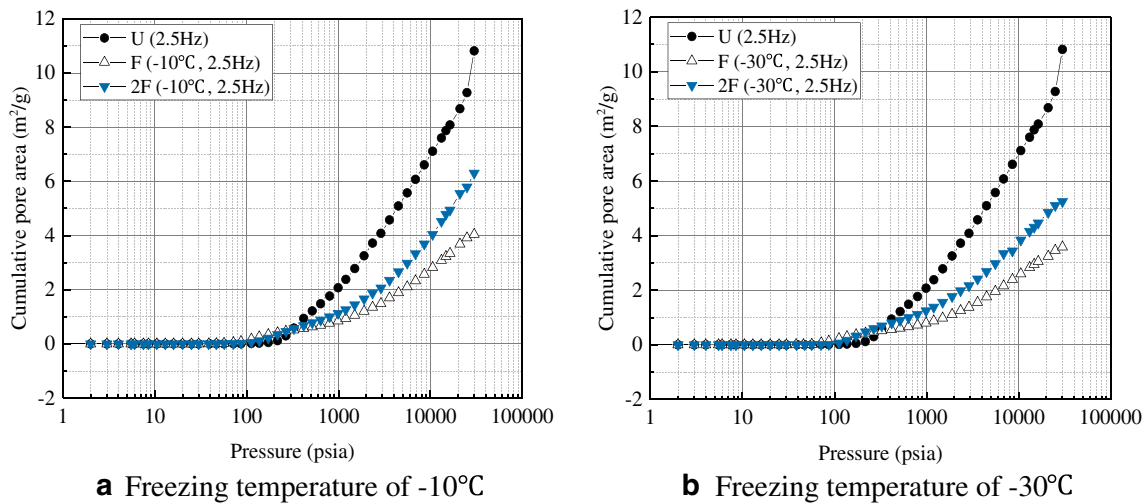


Fig. 14 The cumulative pore area curves at different freezing-thawing cycles. **a** Freezing temperature of $-10\text{ }^{\circ}\text{C}$. **b** Freezing temperature of $-30\text{ }^{\circ}\text{C}$

different diameters can be obtained. From Fig. 11, we can see that the percentage of the pore volume with diameter greater than 800 nm is very small, only about 8%. The pores with diameters between 100 and 10 nm account for a large percentage of volume, which are the main component of the soil. With the decrease of pore diameter, the growth rate of the pore volume percentage is slow in the initial stage with the diameter larger than 800 nm. When the diameters are between 900 and 10 nm, the growth rate increases rapidly, the same as the pore volume. When the diameter is smaller than 10 nm, the percentage of pore volume reaches nearly 100%, this indicates that there are many small pores in the soil. It can be seen from Fig. 11 and Fig. 12 that the curves with different freezing temperatures and freezing-thawing cycles are basically the same except for the stage in which the growth rate is fast.

The variation of cumulative specific surface area of pores with mercury intrusion pressure is similar to that of pore volume. Figure 13 illustrates the variation of cumulative pore area with different freezing temperatures. In the initial stage where the mercury intrusion pressure is less than 100 psi, the

cumulative pore area is almost zero, then the cumulative pore area begins to increase gradually, and the curves show a law of linear growth. Under the same loading condition, the cumulative pore area of undisturbed soil is larger than the thawing soil. It can be seen that the curves of at different freezing temperatures are very close, which is consistent with the conclusion of Zhang and Cui (2018a). The cumulative pore area curves at different freezing-thawing cycles are shown in Fig. 14. We can see that the cumulative pore area of two freezing-thawing cycles is larger than the one freezing-thawing cycle. Generally, the change of the curve is relatively flat, it also indicates that the mercury enters into the large pores first, followed by the small pores, and the number of small pores is large, and macro pores are very few.

The differential pore volume curves at different freezing temperatures are shown in Fig. 15. The trend of each curve is very similar; it gradually reaches the peak value as the pore diameter increases and then gradually decreases. It can be seen that the pore volume has two peaks, and the peak indicates that the pore volume corresponding to the diameter at this point is

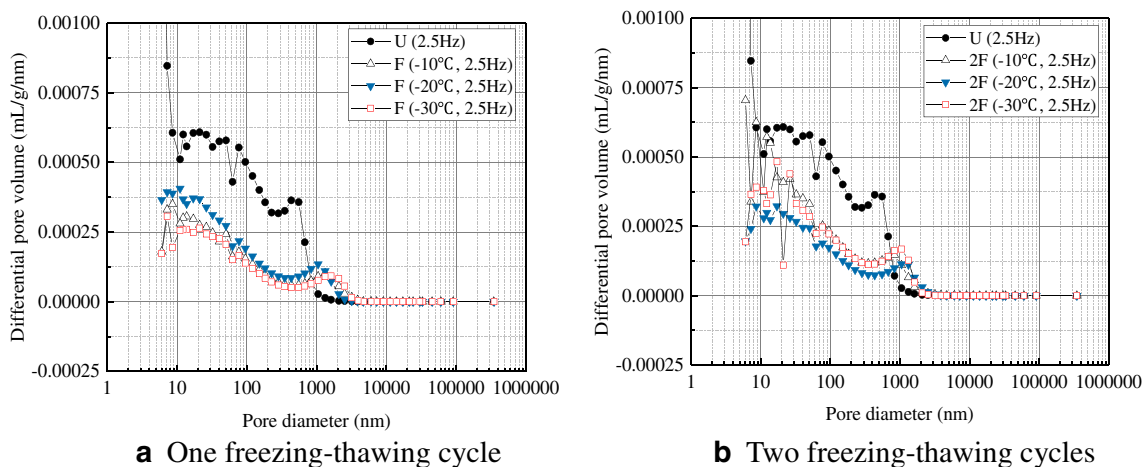


Fig. 15 The differential pore volume curves at different freezing temperatures. **a** One freezing-thawing cycle. **b** Two freezing-thawing cycles

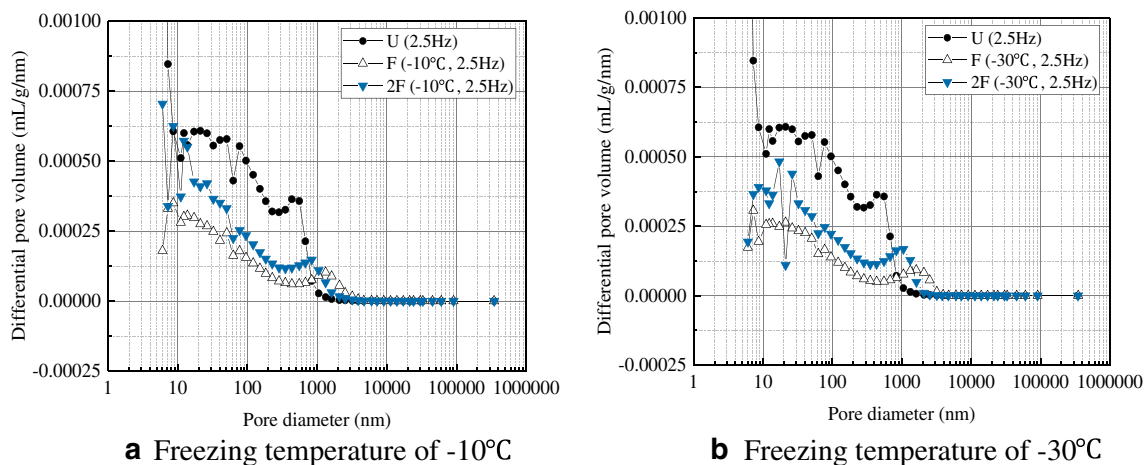


Fig. 16 The differential pore volume curves at different freezing-thawing cycles. **a** Freezing temperature of -10°C . **b** Freezing temperature of -30°C

the largest. The pore volume distribution curves with pore diameter greater than 3000 nm are almost zero, indicating that the distribution of the pore diameters is dominated by smaller pores. Figure 16 presents the differential pore volume curves at different freezing-thawing cycles. We can see from Fig. 15 and Fig. 16 that the curves with different freezing temperatures and freezing-thawing cycles are similar, and the peak values are also very close; the diameter corresponding to the peak point is about 14 nm. This is because the samples have been consolidated for a long time in the dynamic triaxial test, and under 2 h of loading, the pore size has reached a relatively stable value, the pore diameters of most samples are similar.

The log-differential pore volume curves of samples with different freezing temperatures are presented in Fig. 17. The change of the log-differential pore volume represents the pore size distribution of the soil, and the abscissa value corresponding to the peak point of the log-differential mercury volume curve is called the most probable pore diameter. It means that the pore diameter has the highest probability of appearance. It can be seen from the figures that under the same loading condition, the most probable

pore diameter of the unfrozen soil is about 524 nm, and the thawing soil is about 1050 nm. It indicates that the pore size of the thawing soil is larger than that of the undisturbed soil; this is mainly due to the effect of freezing-thawing cycle. With different freezing temperatures, the most probable pore diameter of each sample is very close, the reason is that the pores in the soil are compressed during the dynamic triaxial test, and the reduction of the pore diameters cannot be determined. Figure 18 shows the log-differential pore volume curves at different freezing-thawing cycles. At the freezing temperature of -20°C , the most probable pore diameter subjected to two freezing-thawing cycles is almost the same with that of one freezing-thawing cycle. This is also caused by the compression of the soil by the dynamic triaxial test.

Conclusions

The main goal of this paper is to study the variation of the accumulated deformation and microscopic pore structures of the deep silty clay subjected to freezing-thawing cycles under

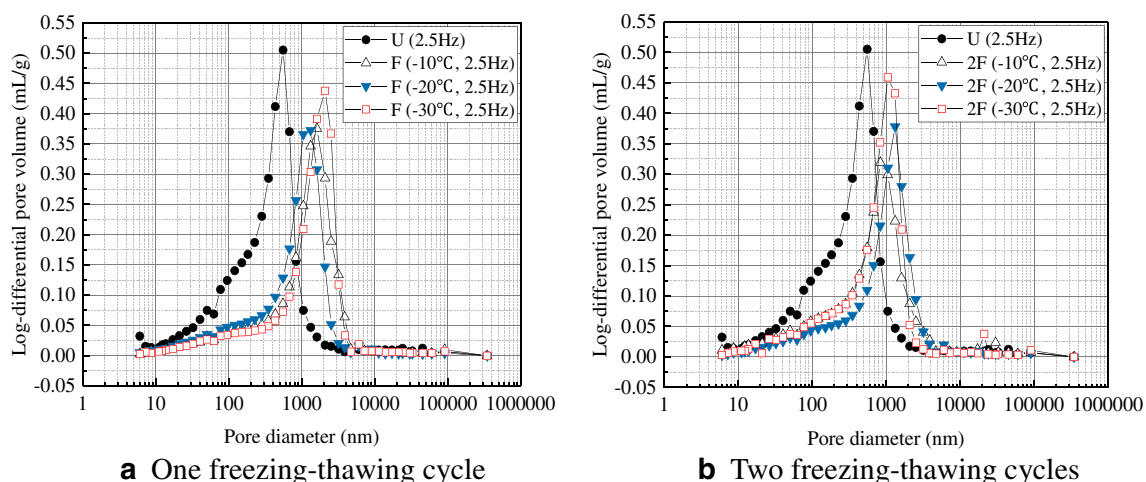


Fig. 17 The log-differential pore volume curves at different freezing temperatures. **a** One freezing-thawing cycle. **b** Two freezing-thawing cycles

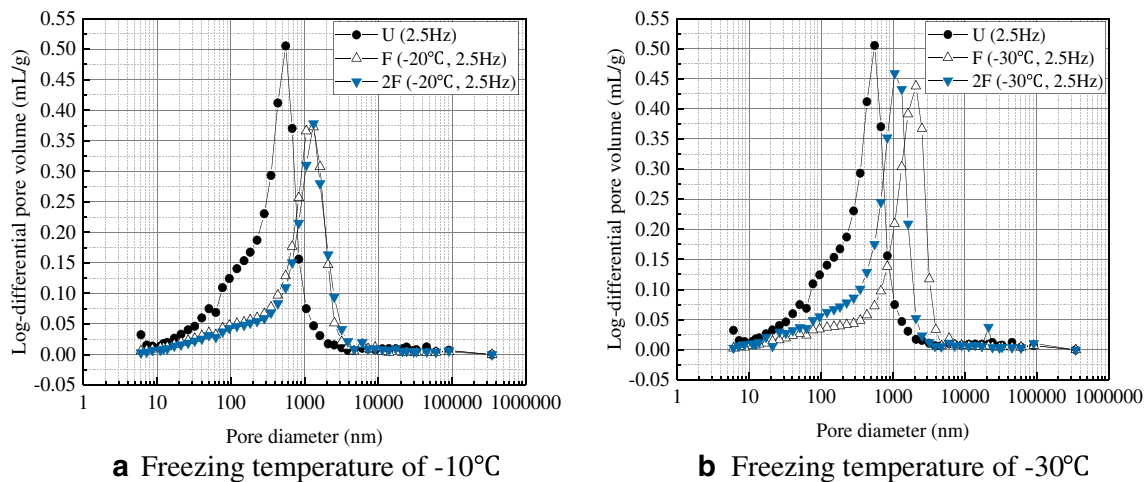


Fig. 18 The log-differential pore volume curves at different freezing-thawing cycles. **a** Freezing temperature of -10°C . **b** Freezing temperature of -30°C

the subway vibration loading. A series of dynamic triaxial tests and MIP test were carried out to study the effects of different vibration frequencies, freezing temperatures, and freezing-thawing cycles. Engineering problems such as accumulated deformation and frost heaving have been observed. The main conclusions are obtained as follows.

1. The accumulated deformation of the silty clay increases with the vibration time increasing, and the axial strain is relatively larger in the initial stage. Under the same loading condition, the strain of the soil subjected to one and two freezing-thawing cycle increases by 39.6% and 72.8% comparing with the unfrozen soil. After freezing-thawing cycle, the volume of water in the pores expands, and the internal structure of the soil is destroyed, two freezing-thawing cycles will aggravate this damage. The research results can be used to predict the stress and deformation variation of silty clay around the tunnel during subway operation.
2. With the increase of vibration time, the rates of increasing of the axial strain gradually decrease. The frequency and the freezing temperature have significant influence on the axial strain. The higher the frequency and the lower the freezing temperature, the more deformation produces to the soil. Because at the same vibration time, the higher frequency is, the more energy transferred to the soil is, which develops larger axial strain. It provides a theoretical reference for analyzing the axial deformation of subway tunnel and ground subsidence caused by different factors.
3. There is a bottleneck with the pressure about 100 psi in the mercury intrusion process. After freezing, the effect of frost heaving leads to the expanding of pores and the change of soil structure. Under the same cyclic loading, the lower the freezing temperatures and the more freezing-thawing cycles, the more mercury intrusion

volume and cumulative pore area, the more obvious this change is. This study could be adopted as reference for the failure mechanism of saturated soft clay around the subway tunnel after freezing construction.

4. The most probable pore diameter of the undisturbed soil is larger than the thawing soil, which is about 524 nm and 1050 nm. The pores with diameters between 10 and 100 nm account for a large part. Due to the pores in the soil are compressed during the dynamic triaxial test, the most probable pore diameters of the samples with different freezing temperatures are close to each other. It explains the damage to the internal structure of soil caused by artificial freezing method, and provides a theoretical reference for the design and construction of the subway tunnel, and the soft soil reinforcement in future construction.

Funding information This work in this paper was funded by the national key research and development program (Grant No. 2017YFC1500702) and by the Fundamental Research Funds for the Central Universities (2013QNA44).

References

- Chamberlain EJ, Gow AJ (1979) Effect of freezing and thawing on the permeability and structure of soils. *Eng Geol* 13(1):73–92
- Cui ZD, Tang YQ (2011) Microstructures of different soil layers caused by the high-rise building group in Shanghai. *Environ Earth Sci* 63(1):109–119
- Cui ZD, Zhang ZL (2015) Comparison of dynamic characteristics of the silty clay before and after freezing and thawing under the subway vibration loading. *Cold Reg Sci Technol* 119:29–36
- Cui ZD, He PP, Yang WH (2014) Mechanical properties of a silty clay subjected to freezing–thawing. *Cold Reg Sci Technol* 98:26–34
- Cui ZD, Zhao LZ, Yuan L (2016) Microstructures of consolidated Kaolin clay at different depths in centrifuge model tests. *Carbonates Evaporites* 31:47–60

- Eigenbord KD (1996) Effects of cyclic freezing and thawing on volume changes and permeabilities of soft fine-grained soils. *Can Geotech J* 33(4):529–537
- Guo L, Wang J, Cai YQ, Liu HL, Gao YF, Sun HL (2013) Undrained deformation behavior of saturated soft clay under long-term cyclic loading. *Soil Dyn Earthq Eng* 50:28–37
- Kamei T, Ahmed A, Shibi T (2012) Effect of freeze–thaw cycles on durability and strength of very soft clay soil stabilised with recycled Bassanite. *Cold Reg Sci Technol* 82:124–129
- Lee W, Bohra NC, Altschaeffl AG, White TD (1995) Resilient modulus of cohesive soils and the effect of freeze–thaw. *Can Geotech J* 32(4): 559–568
- Li J, Tang YQ, Yang P, Liu Q (2015) Dynamic properties of freezing–thawing muddy clay surrounding subway tunnel in Shanghai. *Environ Earth Sci* 74(6):5341–5349
- Lin B, Zhang F, Feng DC, Tang KW, Feng X (2017) Accumulative plastic strain of thawed saturated clay under long-term cyclic loading. *Eng Geol* 231:230–237
- Ling XZ, Li QL, Wang LN, Zhang F, An LS, Xu PJ (2013) Stiffness and damping ratio evolution of frozen clays under long-term low-level repeated cyclic loading: experimental evidence and evolution model. *Cold Reg Sci Technol* 86:45–54
- Ma W, Wu ZW, Zhang LX, Chang XX (1999) Analyses of process on the strength decrease in frozen soils under high confining pressures. *Cold Reg Sci Technol* 29(1):1–7
- Penumadu D, Dean J (2000) Compressibility effect in evaluating the pore-size distribution of kaolin clay using mercury intrusion porosimetry. *Can Geotech J* 37(2):393–405
- Pillai RJ, Robinson RG, Boominathan A (2011) Effect of microfabric on undrained static and cyclic behavior of kaolin clay. *J Geotech Geoenviron* 137(4):421–429
- Shen SL, Wu HN, Cui YJ, Yin ZY (2014) Long-term settlement behaviour of metro tunnels in the soft deposits of Shanghai. *Tunn Undergr Space Technol* 40:309–323
- Simonsen E, Janoo VC, Isacsson U (2002) Resilient properties of unbound road materials during seasonal frost conditions. *J Cold Reg Eng* 16(1):28–50
- Tang YQ, Yan JJ (2014) Effect of freeze–thaw on hydraulic conductivity and microstructure of soft soil in Shanghai area. *Environ Earth Sci* 73(11):7679–7690
- Tang YQ, Cui ZD, Zhang X, Zhao SK (2008) Dynamic response and pore pressure model of the saturated soft clay around the tunnel under vibration loading of Shanghai subway. *Eng Geol* 98(3–4): 126–132
- Tang YQ, Zhou J, Hong J, Yang P, Wang JX (2012) Quantitative analysis of the microstructure of Shanghai muddy clay before and after freezing. *Bull Eng Geol Environ* 71(2):309–316
- Watabe Y, Tsuchida T, Adachi K (2002) Undrained shear strength of Pleistocene Clay in Osaka Bay. *J Geotech Geoenviron* 128(3): 216–226
- Yan CL, Tang YQ, Wang YD, Ren XW (2012) Accumulated deformation characteristics of silty soil under the subway loading in Shanghai. *Nat Hazards* 62(2):375–384
- You ZM, Lai YM, Zhang MY, Liu EL (2017) Quantitative analysis for the effect of microstructure on the mechanical strength of frozen silty clay with different contents of sodium sulfate. *Environ Earth Sci* 76(4):143
- Zhang ZL, Cui ZD (2018a) Effects of freezing–thawing and cyclic loading on pore size distribution of silty clay by mercury intrusion porosimetry. *Cold Reg Sci Technol* 145:185–196
- Zhang ZL, Cui ZD (2018b) Effect of freezing–thawing on dynamic characteristics of the silty clay under K0-consolidated condition. *Cold Reg Sci Technol* 146:32–42
- Zhou CB, Zhao XJ, Chen YF, Liao Z, Liu MM (2018) Interpretation of high pressure pack tests for design of impervious barriers under high-head conditions. *Eng Geol* 234:112–121